Propagation measurements of mobile radio channel over sea at 5.9 GHz

Kun Yang*, Ning Zhou*, Andreas F. Molisch†, *Fellow, IEEE*, Terje Røste*, Egil Eide‡, Torbjörn Ekman‡, Junyi Yu§, Fang Li§ and Wei Chen§
*Super Radio AS,NO-0556 Oslo, Norway. Email: kun@superradio.no
†Wireless Devices and Systems Group, Department of Electrical Engineering
Viterbi School of Engineering, University of Southern California, Los Angeles, California, 90089
‡Department of Electronics and Telecommunications
Norwegian University of Science and Technology, NO-7491 Trondheim, Norway
§School of Automation, Wuhan University of Technology, Wuhan, China 430070

***Abstract*—A radio channel measurement campaign with a maximum distance of 2.6 km was performed in China. In this paper, a detailed description of the channel measurement campaign including antenna setups, channel sounder configurations and other related info is given. The received signal level (RSL) is shown and compared with the Plain Earth Loss model (PEL), the ITU-R P.1546-2 model (ITU-R) and the Round Earth Loss model (REL). It can be found that the REL model matches the measured RSL best according to the values of the Root Mean Square Error (RMSE). The Power-delay profiles (PDPs) are demonstrated, from which the mean excess delay and the RMS delay spread are extracted. It can be found that the 90% of the mean excess delay and the RMS delay spread are within 4.3 ns and 113.3 ns according the corresponding Cumulative Distribution Functions (CDF), respectively. The Akaike Information Criterion (AIC) is used to estimated the best-fit amplitude distribution of the small-scale fading. The Two-Wave with Diffuse power (TWDP) model is found to be the best-fit model with more than 90% incident percentage in the whole route.**

I. Introduction

Digitalization in the ocean industry is considered as one of the most important trends in the maritime nations like Norway, South Korea, China, Singapore, Japan, etc. The digitalization of numerous maritime activities including oil exploitation, maritime transportation, fish farming and other activities drives the needs of broadband maritime communication technology. Since the most of the maritime activities occur within the exclusive economic zone (EEZ) of a country defined as an area extending to a distance of 200 nautical miles (370.4 km) from its costal baseline, the land-based maritime communications with high stability and throughput, large area coverage and comparable low cost, become very attractive to the related markets. On the other hand , the IEEE 802.11p at 5.9 GHz is considered as a candidate for Intelligent Transportation Systems (ITS), which is also related to the maritime transportation. In addition, adjacent frequency bands around 5.862 GHz have been granted for maritime broadband service by the Norwegian Communication Authority [1]. Therefore, the research of radio propagation over sea at 5.9 GHz is essential for the system design, improvement and optimization in maritime environments.

Previously, numerous measurement campaigns by using channel sounders were performed at 1.9 GHz [2], 2.1 GHz [3], and 5.2 GHz [4] respectively. However, the radio channel measurement campaign by using channel sounder at 5.9 GHz has not been performed yet. In addition, some channel measurements have been performed on fixed point-to-point links over sea at 2.4 GHz for a wireless LAN system [5], at UHF bands for a terrestrial digital TV system [6] and at 5.8 GHz for a bouy-to-ship scenario [7], respectively. The resolutions of these measurement solutions for the channel characteristics are limited compared with a channel sounder. On the other hand, the classic PEL model [8], ITU-R model [9] and REL model [10] have not been validated by measurement data at 5.9 GHz in other literatures. To fill these above gaps, a measurement campaign over sea at 5.9 GHz was initialed in MAMIME project [11] founded by Norwegian Research Council and performed in China. In particular, this paper makes the following contributions: it

1) Describes the measurement campaign at 5.9 GHz in China.
2) Presents results from an extensive measurement campaign and compares path loss measurements to the theoretical models.
3) Investigates the PDPs and extracts the CDF of the mean delay and the RMS delay spread.
4) Investigates the small-scale fading distribution as a function of the distance between TX and RX.

The rest of the paper is organized as follows: In section II the measurement campaign is described briefly. In section III the path loss results obtained from the measured data are given, and a comparison with three classic path-loss models is presented in order to identify the best-fit path loss model. Section IV is devoted to the analysis of the power-delay profiles and CDFs of the mean delay and the RMS delay spread. Section IV is devoted to the estimation and parameterization of the small-scale fading. Finally, conclusions are drawn in section V.

II. The measurement campaign

The channel sounder measurement equipment comprising a transmitter (TX) and a receiver (RX) that was provided Super Radio AS, emits a 100 MHz chirp signal at 5.9 GHz. The maximum supported Doppler frequency bands were $\pm$967 Hz. A detailed description of the channel sounder is given in [12]. The measurement campaign was set up for the harbor environment. The RX was installed on the ship and connected with a vertically polarized dipole antennas with 10 dBi gain . The antenna height above sea level is 3.1 m without taking the tidal wave height changes into consideration, (see Fig. 1(a)). A sector antenna with 16 dBi gain was mounted at the TX side on the ship anchored in the middle of the Bay and the antenna height was about 3.1 m above sea level (see Fig. 1(b)). The beamwidths of both antennas are specified in the TABLE I. A dedicated GPS was utilized to record the position data and vessel speed. The ship was traveling along a 2.6 km route (shown in the Fig. 2) in the bay area at a stable speed. Since most of possible reflectors in land are over 1 km away, the reflected paths will be limited and weak at 5.9 GHz. To summarize, the main measurement parameters can be found in the TABLE I.

(a) The RX antenna at the ship.

(b) The TX antenna at the ship anchored in the middle of the bay.

Fig. 1. Receiver and transmitter antennas of the channel sounder

III. The Path loss result and the comparison with different path-loss models

Path loss measurements can be used to validate the path-loss models and adjust the corresponding model parameters, which are very important to improve the accuracy of link budget analysis and radio coverage predictions. In the maritime radio propagation environments, fewer reflectors and scatters exist compared with the urban environment, which makes the radio channel change not very fast. However, the sea wave movements on the reflected and scattered radio waves, and the movement of the ship (both the boat speed and the movements caused by the sea waves) will still make the radio channel variant. To average the small-scale fading, a window of 10 wavelengths, is used and a threshold of 6 dB above the noise floor is implemented to filter out the noise and week reflected waves. It also needs to be mentioned that the RSL measurements include noise and some reflections from the land and surrounding ships (shown in Fig. 4 in Section IV), since the measurement route was not far from the coastline.

The measured RSL is shown in Fig. 3, from which several 'large-scale' fading dips are found at short TX-RX distances (within 500 m), which have also been pointed out in [13], [14], [15]. These fading dips can be up to 25 dB, which can be 'propagation holes' to decrease the system performance dramatically. Small RSL variations (up to 5dB) can be found, which can not be averaged out within the 10 wavelength window. It is mainly caused by the antenna mismatch due to the boat movement and also described in [16]

The obtained RSL is used to compare with the classic

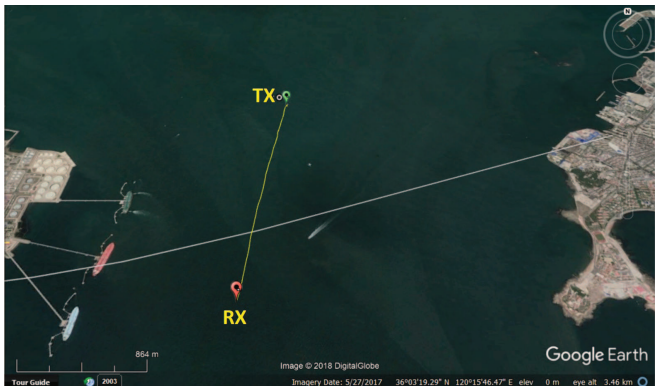

Fig. 2. The route of the ship.

TABLE I
The measurement parameters

Carrier frequency	5.9 GHz
Chirp bandwidth	100 MHz
Transmitting power at the antenna port	16 dBm
Maximum delay span	25.6 μs
Delay resolution	10 ns
Maximum Doppler shift span	$\pm$967 Hz
Number of TX antennas	1
Number of RX antennas	1
TX Antennas beamwidths	$90°(Az.) \times 8°(El.) Approx$
RX Antennas beamwidths	$360°(Az.) \times 11°(El.) Approx$
TX antenna height	3.1 m
RX antenna height	3.1 m
TX antenna gain	16 dBi
RX antenna gain	10 dBi
Cable loss in total	6.5 dBi
Maximum route distance	2.6 km
Temperature	35°C

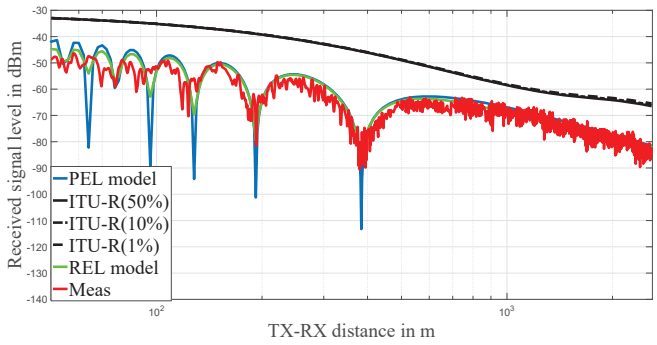

Fig. 3. Comparison between our measurements and three channel models.

TABLE II
THE RMSE RESULTS

Models	Values
PEL model	3.4821
ITU-R (50%)	15.7855
ITU-R (10%)	15.9945
ITU-R (1%)	16.2958
REL MODEL	2.5779

empirical models like the PEL model, the ITU-R model and the REL model (see Fig. 3). The predicted RSLs P_{RX} by different path-loss models are calculated as follows:

$$P_{RX} = P_{TX} + G_{TX} + G_{RX} - L_{cable} - L_{pathloss} \quad (1)$$

where the L_{cable} is the loss of the cable from the RX antenna to the LNA of the RX equipment. The G_{TX} and G_{RX} are the antenna gains at the TX and RX side, respectively. The P_{TX} represents the TX transmitted power from the antenna port. The $L_{pathloss}$ denotes the predicted path loss in dB by different path-loss models where the model parameter values are set according to TABLE I. The Root Mean Square Error (RMSE) as a low-complexity comparison metric for model selection [17], [18] is used to evaluate the difference between the theoretical model and the measured data. It can be found in TABLE II that the RMSE value of the REL model is the smallest, which means it matches the measurements best at 5.9 GHz. This conclusion is consistent with the similar comparisons at 1.4 GHz [19] and 2.1 GHz [10].

IV. POWER-DELAY PROFILE, MEAN DELAY AND RMS DELAY SPREAD

Power delay profile (PDP) is defined as power spectral density in delay domain, which shows the power distribution from different delay bins and can be obtained from the channel impulse response (CIR) $h(t,\tau)$ expressed by using:

$$h(t,\tau) = \sum_k \alpha_k(t)\delta(\tau - \tau_k) \quad (2)$$

where $\alpha_k(t)$ denotes the time-varying complex coefficients for each delay path and τ_k represents the delay time of kth delay path. The instantaneous PDP $P(t,\tau)$ can be expressed by using:

$$P(t,\tau) = |h(t,\tau)|^2 = \sum_k |\alpha_k(t)|^2 \delta(\tau - \tau_k) \quad (3)$$

to simplify the channel description, the moments of the PDP are analyzed on the assumption of Wide Sense Stationary and the uncorrelated scatterers (WSSUS), which means the channel is stationary in both time and frequency domain. For the maritime environment, a 10 wavelength window is considered to fulfill the requirements of the WSSUS assumption, since the maritime environment is relatively stable compared to the dense urban areas. The PDPs within these regions (windows) are averaged to reduce the noise and measurement errors and the averaged PDP (APDP) for each WSS region can be calculated as follows:

$$P(\tau) = E\{P(t,\tau)\} \quad (4)$$

where $E\cdot$ is the average operator over t, which is the 10 wavelength window. The averaged PDP for the whole route is shown in Fig.4, from which it can be found that the Line-of-sight (LOS) domains in the delay domain during the whole route and some reflections are shown at short TX-RX distances. There are also some reflectors at the TX-RX distances between 700 m and 1500 m, and between 2200 m and 2400 m, which are due to the passing-by boats.

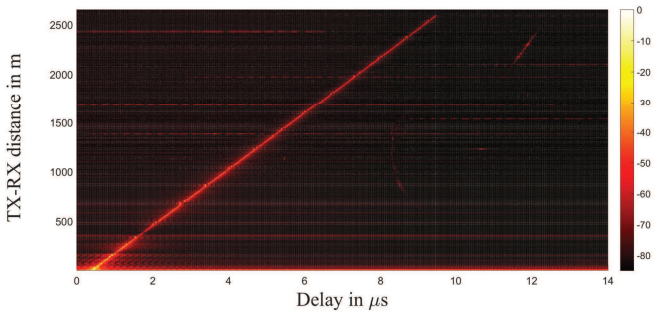

Fig. 4. The averaged PDP for the whole route.

The normalized first-order moment of PDP, the mean delay and the normalized second-order moment of PDP, the RMS delay spread can be expressed by using equation (5) and (6), respectively.

$$T_m = \frac{\int_{-\infty}^{\infty} P(\tau)\tau d\tau}{\int_{-\infty}^{\infty} P(\tau) d\tau} \quad (5)$$

$$S_\tau = \sqrt{\frac{\int_{-\infty}^{\infty} P(\tau)\tau^2 d\tau}{\int_{-\infty}^{\infty} P(\tau) d\tau} - T_m^2} \quad (6)$$

Since the error probability due to delay dispersion is proportional to the rms delay spread [20], the mean excess delay and RMS delay spread can be regarded as a measurement of system performance degradation due to inter-symbol interference (ISI). The RMS delay spread can also be used for system design in terms of the employment of a proper OFDM symbol duration (typically about five time larger than the average RMS delay spread) to avoid the influence of system performance due to the ISI [21]. The statistical properties of the measured mean delay and RMS delay spread are shown by using CDFs

in Fig. 5 and Fig. 6, respectively. From Fig. 5 and Fig. 6, it can be found that the 90% mean excess delay is within 4.3 ns (red circle) and the 90% RMS delay spread (red circle) is within 113.3 ns. These reflections are mainly caused by the surroundings and passing-by boats. It needs to be pointed out that the mean excess delay (up to 1300 ns) and RMS delay (up to 1400 ns) increase dramatically between the range of 2100 m and 2400 m, which is due to a large passing-by ferry in front of our planned measurement route. Therefore, The boat traffic in the harbor or bay areas may make the radio channel frequency selective.

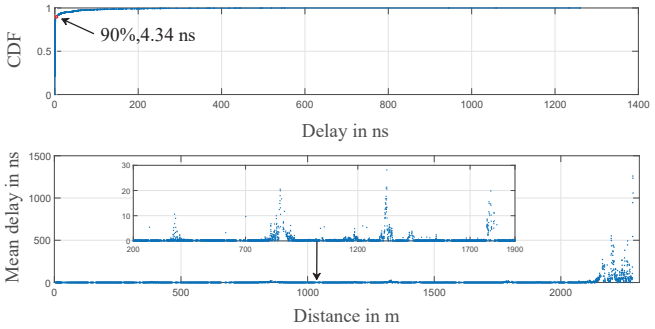

Fig. 5. CDF of mean excess delay.

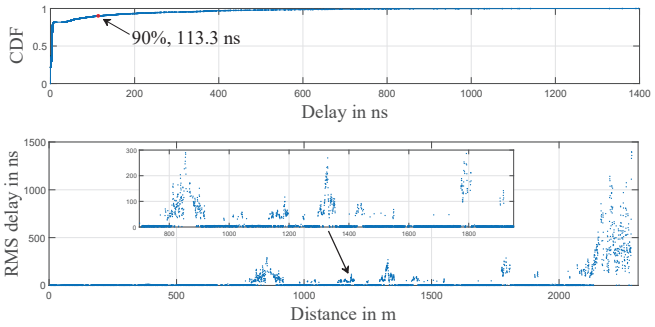

Fig. 6. CDF of RMS delay spread.

V. Small-Scale Channel Properties and the Best-Fit Amplitude Distribution

The properties of the small-scale fading for maritime propagation environments have been studied at 1.9 GHz [2] and 5.2 GHz [4], respectively, which are essential for system design in terms of adaption of modulation scheme, dynamic range, diversity and error-correction coding [22], [23]. Since the radio channel is concluded to be frequency non-selective in the previous section (same conclusion is given at 2.1 GHz in [24]), the amplitude probability density function (PDF) of flat fading is studied based on our measurement data in this section.

A PDF distribution model selection method introduced in [25], [26] is implemented. This model selection method is to select the best functional form based on the Akaike Information Criterion (AIC), whose parameterizations are estimated by maximum-likelihood estimation to match the measured data best. For maritime environments, 6 common distributions including Normal distribution, Rician distribution, Lognormal distribution, Two-Wave with Diffuse power (TWDP) distribution [27], Rayleigh distribution and Weibull distribution, are selected as the relevant functional forms, which have also been used in the data analysis in [4]. It needs to be mentioned that the TWDP and Lognormal distribution are selected due to the ray-tracing geometry and the possible radio link blockages (shadowing) by the passing-by boats, respectively. To filter out the 'large-scale' effect from the original measured data, a window of 10 wavelengths is used for averaging. The best-fit amplitude PDF is estimated from the envelope of the normalized measurements and shown in Fig. 7, where the color-coded gives the best-fit distribution at corresponding TX-RX distances and the overall estimated distribution along the whole boat route is given. It can be found that the TWDP and Rayleigh distribution domain the whole route. The corresponding specific incident percentages can be found in TABLE III, from which it can be concluded that the TWDP can be used as the best-fit amplitude PDF due to more than 90% incident rate. However, it is difficult to find the correlation between the TX-RX distances and other distributions (Rayleigh and Weibull). Therefore, further analysis is needed.

TABLE III
The Percentage of Best-Fit Distribution

TWDP distribution	90.66 %
Rayleigh distribution	9.23 %
Weibull distribution	0.11 %
Normal distribution	0 %
Lognormal distribution	0 %
Rician distribution	0 %

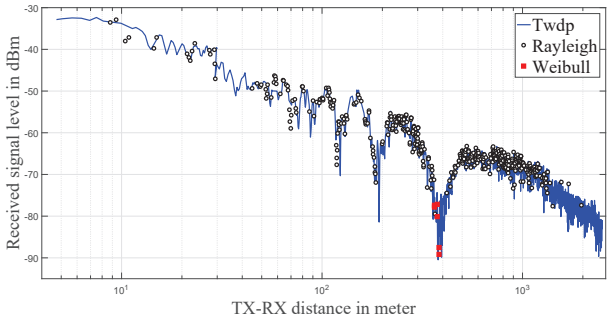

Fig. 7. Overall estimated best-fit distribution.

VI. Conclusions

A channel measurement campaign at 5.9 GHz within a total distance of 2.6 km has been carried out for harbor environments in China. A detailed measurement description is given, which includes the sounder configurations, measurement setups and antenna characteristics. Several 'large-scale' fading dips at short TX-RX distances (within 500 m) and Small RSL variations (up to 5dB) caused by the antenna mismatch due to the boat movement are found in the measured RSL. The measured RSLs are compared to the predicted RSLs

by the three classic propagation models, and it is found that it matches the REL model best according the RMSE value. The APDP of the whole route is obtained from the measured data, from which the mean delay and the RMS delay spread are extracted. It can be found that the 90% mean excess delay and the 90% RMS delay spread are within 4.3 ns and 113.3 ns, respectively. Some significant reflections can be introduced by the surroundings and nearby boat traffics in the harbor and bay areas. The AIC model selection method is implemented to estimate the best-fit amplitude PDF among the proposed 6 common distributions. Only the TWDP, Rayleigh and Weibul model turn out to be the best-fit distribution according to the estimated results, among which the best-fit incident percentage of the TWDP model is the highest (over 90%). There is no clear relation between the positions and the incidence of the distribution models. For simplification, the TWDP model can be used as the amplitude PDF model for the whole route.

ACKNOWLEDGEMENT

We would like to express our sincere thanks to Super Radio AS for providing their channel sounder, and to Ningbo ALLMEAS Tech Co. Ltd and Wuhan University of Technology (WHUT) for performing the measurement campaign. The work of Kun Yang, Ning Zhou, Torbjörn Ekman, Egil Eide, Terje Røste, Junyi Yu was supported by the MAMIME project under Grant Agreement No. 256309 by the Norwegian Research Council. The work of A. F. Molisch was supported by the National Science Foundation. In addition, the work of Fang Li was supported in part by the Young Scientists Fund of National Natural Science Foundation of China (no. 61701356), and in part by the Fundamental Research Funds for the Central Universities (no. 2017-JL-004 and no. 2018III059GX)

REFERENCES

[1] "Utrekna sektoravgift og gebyr for frekvenslyve 2018", Norwegian Communication Authority, 2018

[2] K. N. Maliatsos, P. Loulis, M. Chronopoulos, P. Constantinou, P. Dallas and , M. Ikonomou , "Measurements and Wideband Channel Characterization for Over-the-sea Propagation ," in *IEEE International Conference on Wireless and Mobile Computing, Networking and Communications, 2006. WiMob 2006*. Montreal, Canada, Jun. 2006.

[3] K. Yang, T. Røste, F. Bekkadal, K. Husby and O. Trandem "Long-distance propagation measurements of mobile radio propagation for the open sea at 2 GHz," *IEEE VTC Spring*, San Francisco, US, Sep. 2011.

[4] W. Wang, R. Raulefs. and T. Jost,"Fading Characteristics of Maritime Propagation Channel for Beyond Geometrical Horizon Communications in C-Band," CEAS Space Journal. 10.1007/s12567-017-0185-1, 2017,

[5] N. Fuke, K. Sugiyama, and H. shinonaga, "Long-range oversea wireless network using 2.4 GHz wireless LAN installation and performance ," *proc. The 12th International Conference on Computer Communications and Networks, 2003. IEEE ICCCN 2003*, pp. 351–356, 2003.

[6] M. Nishi, T. Iwami, S. Takahashi and T. Yoshida, "Measurements on UHF radio propagation over the Seto Inland Sea ," *Microwave Conference, 2006. APMC 2006. Asia-Pacific* , pp. 1847–1850, 2006.

[7] J. C. Reyes-Guerrero, L. A. Mariscal, M. Bruno, A. Medouri, "Buoy-to-ship experimental measurements over sea at 5.8 GHz near urban environments", in *Mediterranean Microwave Symp.,(mms11)*. pp. 320-324, September 2011.

[8] S. R. Saunders and A. Aragon-zavala, *Antennas and Propagation for Wireless Communication Systems*. . John Wiley & Sons, 2007.

[9] ITU-R Recommendation P.526-13 (2013), "Propagation by diffraction," Aug. 2014.

[10] K. Yang, A. F. Molisch, T. Ekman and T. Røste "A Deterministic Round Earth Loss Model for Open-Sea Radio Propagation," *IEEE VTC Spring*, 2013 IEEE 77th, Dresden, 2013, pp. 1-5. doi: 10.1109/VTC-Spring.2013.6691821.

[11] http://www.superradio.no/a/home/NATIONAL/

[12] F. Li, W. Chen, Y. Shui, L. Xu, J. Y. Yu, C. Li, K. Yang, F. Chang, "5.9 GHz vehicular channels comparisons between two traffic status for dense urban area," in special issue on *Wireless Communication over ZigBee for Automotive Inclination Measurement*, China Communications 15(4):58-71 April 2018

[13] K. Yang, T. Røste, F. Bekkadal and T. Ekman, "Land-to-ship radio channel measurements over sea at 2 GHz," in *IEEE International Conference on Wireless Communications, Networking and Mobile Computing, 2010. WICOM2010*. Chengdu, China, Sep. 2010.

[14] K. B Kim, A. Maifuz, J. H. Lee, S. O. Park "Experimental Study of Propagation Characteristic for Maritime Wireless Communication," in *International Symposium on Antennas and Propagation (ISAP2012)*. Nagoya, Japan, Nov. 2012.

[15] W. Wang, G. Hoerack, T. Jost, R. Raulefs, M. Walter, U. C. Fiebig, "Propagation channel at 5.2 GHz in baltic sea with focus on scattering phenomena," in *9th European Conference on Antennas and Propagation (EuCAP)*. Paris, France, May. 2015.

[16] K. Yang, T. Røste, F. Bekkadal and T. Ekman, "Channel characterization including path loss and Doppler effects with sea reflections for mobile radio propagation over sea at 2 GHz ," in *IEEE International Conference on Wireless Communications and Signal Processing, 2010. WCSP 2010*. Suzhou, China, Oct. 2010.

[17] M. Farhoud, A. El-Keyi, A. Sultan, "Empirical correction of the Okumura-Hata model for the 900 MHz band in Egypt," Third International Conference on Communications and Information Technology (ICCIT), pp 386-390, 2013.

[18] R. Ignacio, C. Nguyen. Huan , et al."A Geometrical-Based Vertical Gain Correction for Signal Strength Prediction of Downtilted Base Station Antennas in Urban Areas," In Vehicular Technology Conference (VTC Fall), pp 1-5, 2012.

[19] J. Y. Yu, W. Chen, K. Yang, C. Li, F. Li, Y. Shui "Path loss channel model for inland river radio propagation at 1.4 GHz," in *International Journal of Antennas and Propagation*, 2017

[20] A. F. Molisch, *Wirless Communications*. . John Wiley & Sons, 2007.

[21] T. Ganesh, K. Pahlavan "Statistics of short time and spatial variations measured in wideband indoor radio channels ," *IEE proceedings-H, Vol.140, No.4*, Aug, 1993.

[22] E. Biglieri, J. Proakis and S. Shamai, "Fading channels: information-theoretic and communications aspects," IEEE Transactions on Information Theory, vol.44, no.6, pp.2619-2692, Oct 1998,

[23] M. K. Simon and Mohamed-Slim Alouini, "Digital communication over fading channels," Vol. 95. John Wiley & Sons, 2005.

[24] K. Yang, T. Røste, F. Bekkadal, and T. Ekman "Experimental multipath delay profile of mobile radio channels over sea at 2 GHz," *IEEE LAPC*, loughborough, UK, Nov. 2012.

[25] U. G. Schuster and H. Bolcskei, "Ultrawideband Channel Modeling on the Basis of Information-Theoretic Criteria.", *IEEE Trans. on WIRELESS COMMUNICATIONS.* vol. 6, no. 7, pp. 2464–2475, July. 2007.

[26] C. C. Chong and S. K. Yong, "A Generic Statistical-Based UWB Channel Model for High-Rise Apartments.", *IEEE Trans. on Antenna and Propagation.* vol. 53, no. 8, pp. 2389–2399, Aug. 2005.

[27] G. D. Durgin, T. S. Rappaport and D. A. de Wolf, "New Analytical Models and Probability Density Functions for Fading in Wireless Communications.", *IEEE Trans. on WIRELESS COMMUNICATIONS.* vol. 50, no. 6, pp. 1005–1015, June. 2002.